Nanoscale

Improved and targeted delivery of bioactive molecules to cells with magnetic layer-by-layer assembled microcapsules

Journal:	*Nanoscale*
Manuscript ID:	NR-ART-02-2015-001261.R1
Article Type:	Paper
Date Submitted by the Author:	21-Apr-2015
Complete List of Authors:	Pavlov, Anton; Queen Mary University of London, School of Engineering & Materials Science Gabriel, Samantha; Queen Mary, University of London, School of Engineering and Materials Science Sukhorukov , Gleb; Queen Mary, University of London, School of Engineering and Materials Science Gould, David J.; Queen Mary University of London, Bone & Joint research Unit

SCHOLARONE™
Manuscripts

Journal Name

RSCPublishing

ARTICLE

Improved and targeted delivery of bioactive molecules to cells with magnetic layer-by-layer assembled microcapsules

Cite this: DOI: 10.1039/x0xx00000x

Received 00th January 2012,
Accepted 00th January 2012

DOI: 10.1039/x0xx00000x

www.rsc.org/

Anton M. Pavlov[†a,b], Samantha A. Gabriel[†a], Gleb B. Sukhorukov[a*], David J. Gould[c]
,

Despite our increasing knowledge of cell biology and the recognition of an increasing repertoire of druggable intracellular therapeutic targets, there remain a limited number of approaches to deliver bioactive molecules to cells and even fewer that enable targeted delivery. Layer-by-layer (LbL) microcapsules are assembled using alternate layers of oppositely charged molecules and are potential cell delivery vehicles for applications in nanomedicine. There are a wide variety of charged molecules that can be introduced in the microcapsule structure including metal nanoparticles that introduce physical attributes. Delivery of bioactive molecules to cells with LbL microcapsules has recently been demonstrated, so in this study we explore the delivery of bioactive molecules (luciferase enzyme and plasmid DNA) to cells using biodegradable microcapsules containing a layer of magnetite nanoparticles. Interestingly, significantly improved intracellular luciferase enzyme activity (25 fold) and increased transfection efficiency with plasmid DNA (3.4 fold) was observed with magnetic microcapsules. The use of a neodymium magnet enabled efficient targeting of magnetic microcapsules which further improved the delivery efficiency of the cargoes as a consequence of increased microcapsule concentration at the magnetic site. Microcapsules were well tolerated by cells in these experiments and only displayed signs of toxicity at a capsule:cell ratio of 100:1 and with extended exposure. These studies illustrate how multi-functionalization of LbL microcapsules can improve and target delivery of bioactive molecules to cells.

Keywords: LbL, microcapsules, intracellular delivery, magnetic targeting, protein, enzyme, luciferase, gene delivery.

Introduction

LbL assembly is performed under native conditions which are compatible for the inclusion of bioactive molecules in assembled microcapsules or other structures such as cellular coatings [1]. Intracellular delivery of bioactive species has tremendous potential for clinical application as well as investigating behaviour of various molecules in their natural state inside cells [2-5]. LbL-assembled microcapsules are interesting vehicles to use in cell delivery because a variety of biological or physical properties which can endow them with multifunctionality [6, 7]. Physical characteristics can be added to LbL microcapsules through inclusion of metal nanoparticles into the shells. Gold nanoparticles have been employed to trigger intracellular release of molecules in response to laser-induced heating [8-12], and magnetic nanoparticles have been employed for magnetically controlled targeting. Studies have shown that magnetic microcapsules can be moved to a magnet [13, 14], whilst motorized microcapsules can be directed to a magnet [15]. Cellular studies have demonstrated that ligand bound magnetic microcapsules can be employed to sort cancer cells [16] and cells with internalized magnetic microcapsules that are either adherent or in suspension can be navigated with a magnet [17, 18]. Whilst under flow conditions magnetite containing microcapsules can be magnetically targeted with several microcapsules delivered to each cell [12, 19]. Despite the potential for magnetic microcapsules in targeted cell delivery, no study

has actually examined delivery of bioactive cargo molecules in the absence or presence of a magnetic field.

Delivering bioactive molecules to cells in a targeted manner remains a challenge in the development of novel therapies. Proteins encompass a vast range of molecules including enzymes, hormones, cytokines and transcription factors many of which act inside cells, yet our ability to deliver proteins to cells is very limited. Cell penetrating peptides such as the viral peptides TAT and VP22 have a high percentage of positively charged amino acids and have an ability to directly translocate across the cell plasma membrane and transport fused proteins with them, however, this approach indiscriminately targets all cells unless they are engineered with a targeting moiety[20]. The delivery of nucleic acids to cells uses a wide variety of approaches for genetic modification of cells in tissue culture but *in vivo* delivery is more complex and targeted delivery relies on the natural tropism of viruses or incorporating antibody or peptide targeting domains into chimeric proteins or lipocomplexes. Microcapsules have the ability to deliver both proteins and nucleic acids to cells and indeed through their multifunctionalisation we have demonstrated co-delivery of both [21]. In this study we examined the influence of magnetic nanoparticles on microcapsule delivery and the ability to magnetically target delivery of bioactive molecules.

Materials and Methods

Poly-L-arginine hydrochloride (PLA, molecular weight 15-70 kDa), dextran sulfate sodium salt (DS, molecular weight ~100 kDa), polyethyleneimine, branched (PEI, 25 kDa), ethylenediaminetetraacetic acid disodium salt (EDTA), sodium hydroxide, citric acid monohydrate, ammonium hydroxide, and all salts were purchased from Sigma. Other reagents included recombinant American firefly luciferase (Roche Diagnostics GmbH, Mannheim, Germany), luciferase assay system, D-luciferin K+ salt from Promega Corp (Madison, WI, USA) and Dulbecco's Modified Eagles Media (DMEM), Fetal Bovine Serum (FBS), penicillin and trypsin purchased from Lonza.

Plasmid preparation

Plasmid pcLuc+[22] encoding firefly luciferase from a CMV promoter was propagated in DH5α E. coli and was purified using the Qiagen endofree mega kit (Qiagen Ltd., Crawley, West Sussex, UK) with plasmid DNA re-suspended in sterile distilled water.

Magnetic nanoparticles

Magnetite nanoparticles (FeNP) were synthesized according to the Massart's precipitation method, followed by particle surface functionalization with citric acid[23]. Briefly, 0.86 g $FeCl_2$ and 2.35 g $FeCl_3$ were dissolved in 40 mL of water and heated to 80ºC under argon in a three-necked flask. While vigorously stirring the reaction mixture, 5 mL of NH_4OH was slowly introduced by a syringe and heated for a further 30 min. Next, 1 g of citric acid dissolved in 2 mL of water was introduced, and the temperature was raised to 95ºC. Stirring was continued for a further 90 min. Subsequently, the nanoparticles dispersion was dialyzed against water in a 12-14 kD cut-off cellulose membrane (Carl Roth, Germany), resulting in a stable dispersion of negatively charged magnetite nanoparticles. Particle size and zeta-potential were determined via DLS and electrophoretic mobility measurements, respectively, using Malvern Nano ZS revealing a mean particle size of 30 nm and a zeta potential of –25 mV. Size measurement results were also confirmed by TEM imaging using a JEOL JEM 2010 electron microscope.

Microcapsules

Microcapsules used for experiments were assembled upon calcium carbonate sacrificial templates, according to a well-established protocol [24]. $CaCO_3$ microparticles were synthesized by mixing 0.33M $CaCl_2$ and 0.33M Na_2CO_3 solutions at 1:1 ratio immediately before use. When luciferase or pcLuc$^+$ were incorporated into the cores, this was achieved by their co-precipitation; luciferase or plasmid solutions (at concentration of 1 mg/mL) were mixed with $CaCl_2$ prior to Na_2CO_3 addition. Mass of bioactive compounds used for co-precipitation was kept at ~200 μg per ml of $CaCl_2$, as this ratio was used in our previous studies [21, 25]. After successful core synthesis was verified by optical microscopy, layers were assembled following the usual LbL procedure.

Layers had a structure of $(PLA/DS)_3$/PEI for non-magnetic biodegradable microcapsules and $(PLA/DS)_{1.5}$/FeNP/PLA/DS/PEI for magnetic biodegradable microcapsules. All polyelectrolytes were adsorbed from 2 mg/ml solutions. Molarity of NaCl solution used as the solvent for polyelectrolytes was 0.15 M for biodegradable polyelectrolytes and 0.5 M for PEI. FeNP incorporation was achieved due to strong electrostatic interaction between positively charged groups of PLA and negatively charged citrate groups of nanoparticles. Nanoparticles were adsorbed from excess to fully cover the microcapsule surface to ensure total charge overcompensation which is essential for successful LbL assembly. An outermost layer of PEI was used to enhance enzyme activity and plasmid DNA transfection efficiency through promotion of endosomal escape [21, 26].

After the layers were completed, $CaCO_3$ cores were dissolved in 0.2 M EDTA solution at pH 6.5. Microcapsules obtained had a mean diameter of 3-4 μm, as confirmed by SEM imaging. Microcapsule concentration was measured by haemocytometry and was adjusted to match the microcapsules:cell ratio chosen for each experiment. Microcapsules were resuspended in PBS immediately prior to their addition to cells.

Incorporation ratios of enzyme and plasmids were determined by measuring the concentration of corresponding species in supernatants collected from microcapsule synthesis following the same procedure as described previously[21]. Luciferase concentration measurements were performed using an MLX Microtiter® Plate Luminometer (Dynex Technologies Inc., USA) and a calibration curve obtained using the solution of luciferase used for co-precipitation. Plasmid DNA concentrations were measured using Qubit™ dsDNA HS Assay

 This journal is © The Royal Society of Chemistry 2012

Kits with the Qubit® 2.0 Fluorometer (Invitrogen). Concentration measurements were performed on centrifuged (4000 rpm, 5 min) solutions. Measured incorporation ratios were similar to previously reported values[21].
Microcapsule structure was characterised by scanning electron microscopy using FEI Inspect F electron microscope. For sample preparation, a drop of microcapsule dispersion was put on top of a small glass slide attached to the sample holder and sputtered with gold after drying. Images were taken using an acceleration voltage of 10 kV.

Cell culture and cell viability tests

The human embryonic kidney epithelial cell line 293T, human epithelial carcinoma cell line HeLa were grown in DMEM supplemented with penicillin (100 U/ml), streptomycin (100 µg/ml) glutamine (2 mM) and 10% FBS, in a humidified incubator containing 10% CO_2 at 37°C.
For cell viability studies HeLa cells were plated at 30,000 cells per well on 96 well plates. The next day microcapsules were added at ratios of 10 and 100 capsules per cell to triplicate wells and on the subsequent 2 days microcapsules were added at the same ratios to additional wells. The experiment was terminated 24 hours later when total incubation times reached 24, 48 and 72 hours for respective wells. Then 100 µl titreGLO assay reagent (Promega Corp) was added to each well, plates were briefly shaken and then incubated for 20 minutes before the luminescent signal in 1 second was recorded using a plate luminometer.

Microcapsule delivery to cells

Cells were plated in 24 or 96-well plates at the density described in individual experiments. The following day 10 µL of microcapsule suspension was introduced at cell:microcapsule ratios in the range of 1:0.625 to 1:10. In experiments investigating the influence of a magnetic field on delivery, a magnet (25 x 10 x 3mm thick N42 Neodymium Magnet, First4Magnets.com, Nottinghamshire, UK) was either placed under the whole well or the left half of the well during microcapsule addition. When a continuous magnetic field was used a smaller magnet (10 x 3.5 x 2.25mm thick N45 Neodymium Magnet, e-magnetsuk.com) was placed under the left side of the well during addition and it remained in place for the duration of the experiment.

Sedimentation rate of microcapsules

The rates of sedimentation of magnetic and standard microcapsules were monitored using a PerkinElmer Lambda 35 spectrophotometer by measuring absorbance of 3 ml microcapsule dispersions at matched concentrations in 4.5 ml spectrometry cuvettes at 328 nm at regular time intervals. The wavelength was chosen as a peak for adsorption by magnetic nanoparticles. To measure the sedimentation rate of magnetic microcapsules in a magnetic field, the N45 magnet was placed under the base of the cuvette.

Luciferase activity assay

Cell lysates were prepared from triplicate wells by addition of passive lysis buffer (Promega Corp) for 15 minutes at 37 °C. Lysates were then collected and stored frozen (-20 °C) until analysis for enzyme activity. Luciferase activity was monitored by standard luminometry following addition of 50 µl of luciferase assay reagent (Promega Corp) to cell lysate (10 µl). Light emission was monitored for 10 seconds following addition of substrate (50 µl) with an MLX Microtiter® Plate Luminometer (Dynex Technologies, USA).

Bioluminescence Imaging

Real-time bioluminescent imaging was performed with an IVIS 100 system (PerkinElmer Inc. Waltham, MA, USA) which was used to monitor the uptake of luciferase enzyme containing microcapsules into 293T cells or their transfection with plasmid DNA containing microcapsules. These experiments were performed in black tissue culture plates (Visiplate™ TC, PerkinElmer Inc.) twenty seconds prior to the imaging 12.5 µl of D-luciferin K+ salt (Promega Corp) was added to each well, images were collected without further addition of substrate. A black and white photo was taken and this was overlaid with a bioluminescent image. The bioluminescent signal from each well was quantitated using Living Image software version 2.5.50.1 with values expressed as photons per steradian per centimetre squared. Where magnetic targeting was used, a region of interest template was used to determine the bioluminescence of each half of the well or in the area where the magnet was positioned.

Results

Previously we have shown that a middle layer of enzyme or plasmid DNA sandwiched between polyelectrolytes in the microcapsule shell is shielded and ineffective for delivery to cells[21, 25]. However, physical properties have been added to microcapsules through inclusion of metal nanoparticles in a middle layer [13]. In this study we introduced magnetite nanoparticles as a middle layer of biodegradable microcapsules which changed their appearance (Figure 1A and B) but also increased their density resulting in more rapid sedimentation from a microcapsule suspension compared to standard microcapsules and this sedimentation could be further accelerated through use of a magnet (Figure 1C). Importantly, for cell delivery studies, magnetic microcapsules were well tolerated by cells and only displayed toxicity after incubation at a ratio of 100:1 microcapsules per cell for 48 hours or longer (Figure 1D).

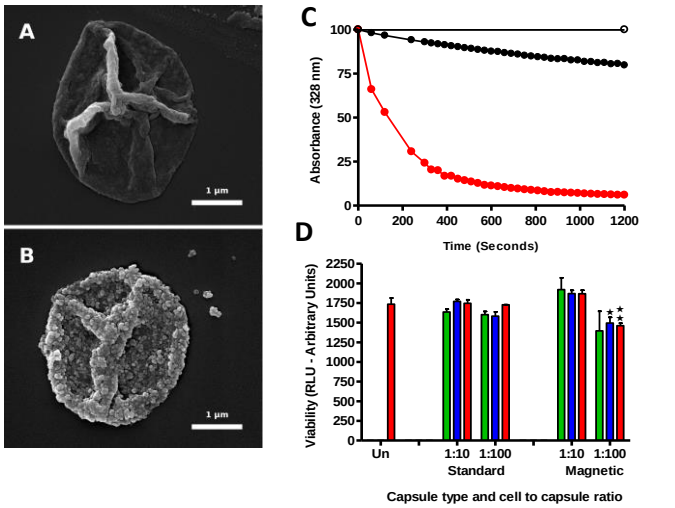

Figure 1. Appearance and properties of magnetic microcapsules. Scanning electron microscope images of a standard (A) and magnetic (B) biodegradable microcapsule. Sedimentation of microcapsules in 20 minutes was monitored by the change in absorbance at 328 nm (C) with standard microcapsules (open circles) and magnetic microcapsules in the absence (solid black circles) and presence of a magnetic field (red circles) shown. Toxicity of magnetic and standard microcapsules to HeLa cells was also monitored (D). Cells were either untreated (Un) or were exposed to microcapsules at ratios of 1:10 or 1:100 for 24 hours (green bars), 48 hours (blue bars) or 72 hours (red bars). Values are the mean of triplicate readings with the SEM shown by the error bar. Significant differences from the untreated cells of $p \leq 0.05$ and $p \leq 0.01$ are shown by ★ and ★★, respectively.

In view of this observation subsequent cell delivery experiments utilised a maximum initial microcapsule:cell ratio of 10:1 or lower. Increased density of microcapsules with magnetic nanoparticles compared to non-magnetic microcapsules enhanced their sedimentation rate, resulting in faster contact of cells with capsules, and hence internalization. When monitored by real-time bioluminescent imaging magnetic microcapsules displayed both improved delivery kinetics and higher maximal delivery of luciferase to cells. After 240 minutes of incubation magnetic microcapsules displayed a 25 fold enhancement in delivery of active luciferase enzyme to cells compared to standard microcapsules (Figure 2A and B).

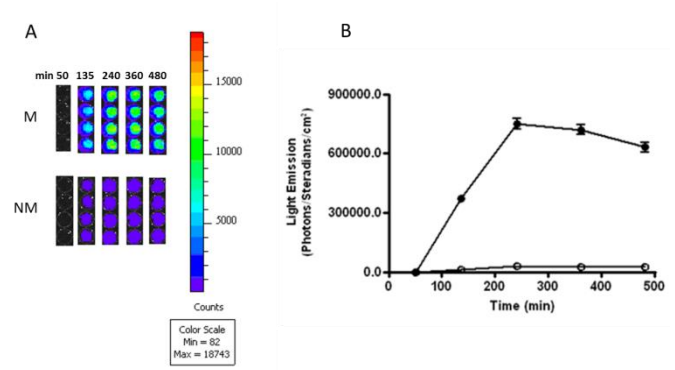

Figure 2. Improved luciferase enzyme delivery with magnetic microcapsules. Magnetic (M, solid circles) and standard (NM, open circles) microcapsules with core luciferase were added to 293T cells in 12 well plates (150,000/well) at a capsule to cell ratio of 10:1 and delivery was monitored by real time bioluminescence imaging at time-points up to 480 minutes (A). Light emission was quantitated with Living Image software version 2.5.50.1 (B). Values are the mean of triplicate readings and vertical lines are the standard error of the mean.

In similar studies, plasmid DNA encoding luciferase enzyme was delivered with both standard and magnetic microcapsules (Figure 3A and B). Again, these experiments demonstrated improved transfection of 293T cells with magnetic microcapsules (by a factor of 3.4 fold after 72 hours with a 10:1 ratio, Figure 3A and B). Interestingly when a static magnet was placed under the whole well during addition of magnetic microcapsules there was no further enhancement of delivery (data not shown).

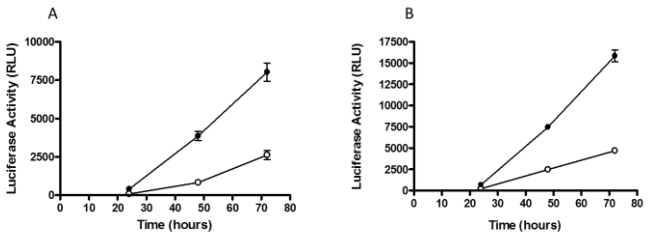

Figure 3. Enhanced cell transfection with magnetic LbL microcapsules. Microcapsules containing pcLuc+ plasmid DNA were added to cells (30,000) in 96 well plates at ratios of 5:1 (A) and 10:1 (B). Cell lysates were collected at 24, 48 and 72 hours after standard (open circle) and magnetic (black circle) microcapsule delivery and luciferase activity in the lysates was measured using a plate luminometer. Values are the mean of triplicate readings and vertical lines are the standard error of the mean.

Whilst magnetic attraction *per se* did not significantly alter cell transfection with magnetic microcapsules we were also interested in exploring the potential of microcapsule targeting with a magnet and studying the effect of this on efficiency of cell delivery. Experiments were performed in wells where the left-hand side was placed on top of a magnet at the time of microcapsule addition (Figure 4A). Experiments with luciferase enzyme containing microcapsules confirmed the ability to target magnetic microcapsules to the left-hand side of the well with significantly more luciferase signal compared to the right-hand side of these wells (Figure 4B and C). If all the microcapsules navigated to the side of the well where the magnet was located this would represent a doubling of the microcapsule to cell ratio on that side. Indeed, the data in Figure 4C generally upholds this hypothesis, with light emission on the left hand side similar to the light emission from each side of the well when a 2 fold higher ratio of the microcapsules to cells was used but without magnetic targeting (Figure 4C).

This journal is © The Royal Society of Chemistry 2012

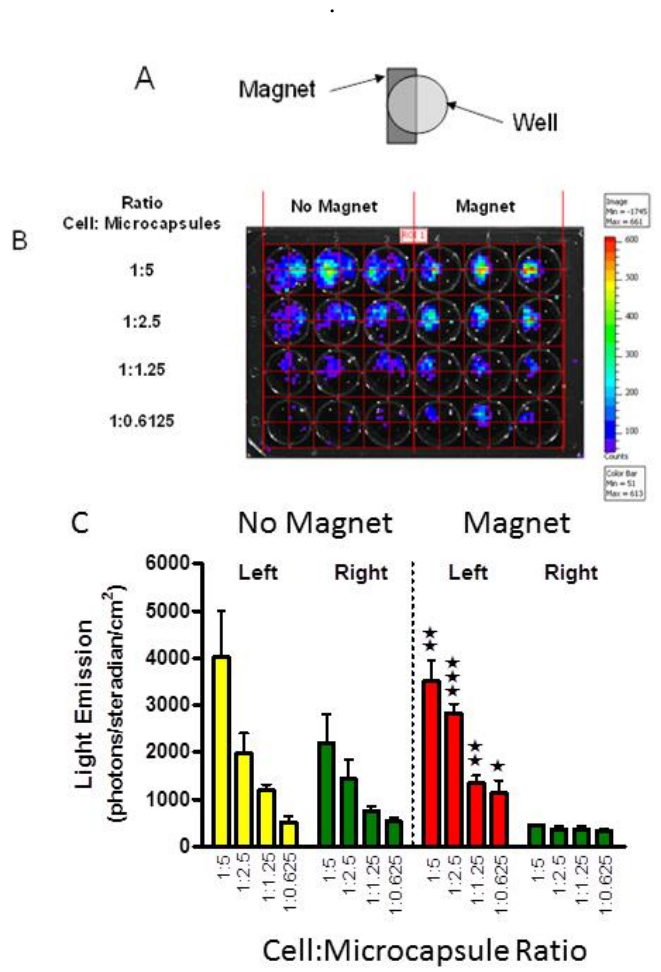

Figure 4. Magnetic targeting of luciferase microcapsules. 293T cells (150,000/well) were plated on a 24 well black walled tissue culture plate. The next day magnetic microcapsules were added to triplicate wells at ratios of 5, 2.5, 1.25 and 0.6125 per cell. At the time of addition either a magnet was placed under the left half of the well (A) or no magnet was used. After 300 minutes potassium luciferase substrate was added to each well and a bioluminescent image was captured on the large pixel setting for 10 minutes (B). Light emission from each well was quantified using the grid template overlaid in B and light emission values for the left and right sides of each well were calculated and mean values of triplicate readings were plotted (C). Vertical lines represent the SEM and significant differences from the right-hand side of the well of p≤0.05, p≤0.01 and p≤0.001 are indicated by ★, ★★ and ★★★, respectively.

We also demonstrated targeted transfection with magnetic microcapsules. In this experiment transfection with magnetic and magnet targeted magnetic microcapsules (Figure 5A) were compared at two ratios (1:1 and 1:10). Targeting was again demonstrated by real-time bioluminescent imaging and is clearly seen in the displayed image (Figure 5B) and plotted data (Figure 5C). The small magnet (surface area 0.35 cm^2) remained under the well for the duration of the experiment and if all the delivered microcapsules located in the area of the magnet this would amount to a concentration increase of 5.4 fold (surface area of the well was 1.9 cm^2). In effect this would equate to a cell to microcapsule ratio of 1:5.4 and 1:54 in the area of the magnet for the 1:1 and 1:10 ratio wells, respectively.

When the magnet was used, the light emission from its site was 7 fold higher than from the rest of the well. These observations confirm that magnetic microcapsules can be targeted with a magnet with a consequent increase in transfection efficiency at the localized site.

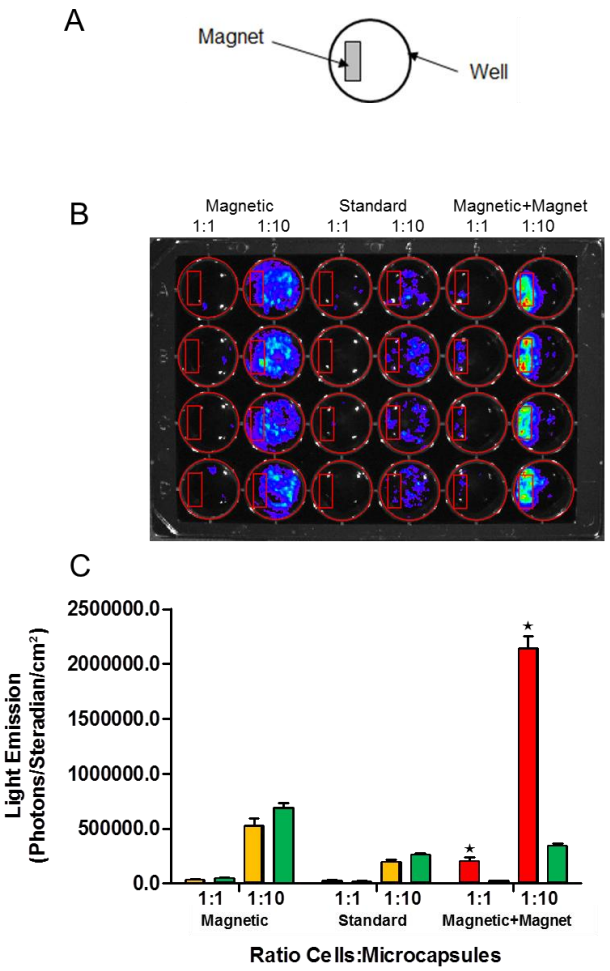

Figure 5. Magnetically targeted microcapsule transfection. 293T cells (150,000/well) were plated on a 24 well black walled tissue culture plate. The next day magnetic microcapsules were added to quadruplicate wells at ratios of cell to microcapsules of 1:1 or 1:10. For indicated wells, a small magnet (A) was placed under the left-hand side of the well at the time of microcapsule addition and remained in place throughout the course of the experiment. After 72 hours potassium luciferase substrate was added to each well and a bioluminescent image was captured on the small pixel setting for 30 seconds (B). Light emission from each well was quantified using the template shown in B so that light emission from the site of the magnet and the rest of the well (both divided by area) were calculated. Mean values of quadruplicate readings were plotted (C) with yellow bars indicating light from the theoretical site of the magnet, red bars representing light from the actual site of the magnet and green bars representing light from the rest of the well. Vertical lines represent the SEM and significant differences between the site of the magnet and the rest of the well of p ≤0.005 are indicated by ★.

Discussion

In these studies we have revealed some interesting aspects of cell delivery of bioactive molecules with magnetic LbL microcapsules. We know from other work that the initial

interaction between standard microcapsules and the cell surface is electrostatic and they are engulfed by a phagocytotic mechanism utilising lipid-raft mediated macropinocytosis which targets microcapsules into acidic heterophagolysosomes [27]. The increased sedimentation rate of magnetic microcapsules will result in more rapid interaction with cells and potentially an increased efficiency of cell delivery which results in improved kinetics of luciferase delivery and cell transfection than achieved with standard microcapsules. An interesting observation is the difference in enhancement of luciferase delivery (x25) and cell transfection (x3.4) with magnetic microcapsules (without a magnet) compared to standard microcapsules. The improvement in cell uptake of microcapsules will be similar for both cargoes so the difference in the magnitude of enhanced activity (enzyme or transfection) must relate to their intracellular processing. Luciferase is an active molecule which can provide signal whilst associated with the microcapsule structure [21] whereas plasmid DNA must be liberated from capsules to enter the nucleus and proceed through transcription and translation before enzyme activity of newly formed protein can be monitored. We also know that plasmid DNA interacts with polyarginine in an almost irreversible manner with the polypeptide located in the DNA minor grove and polypeptide side chains neutralizing phosphate charges of the DNA [28, 29]. Despite better delivery to cells it may well be that liberation of plasmid DNA from microcapsules is impeded by its interaction with this component of the microcapsule structure. Plasmid DNA will also need to transit from the endosome to the cytosol which should be facilitated by the proton sponge effect of PEI. Indeed we have previously used PEI for plasmid DNA delivery from LbL microcapsules [21] and similar microcapsules have utilised PEI to promote delivery of siRNA to cells [30]. Interestingly, the incorporation of PEI into the microcapsule structure for siRNA delivery resulted in a reduction in its toxicity to cells [30]. The increased density alone enables more rapid interaction of magnetic microcapsules with cells so it would be interesting to examine alternative construction approaches that also result in higher density microcapsules, to determine their influence on delivery. Indeed, previous work has shown that increasing the amount of complexed DNA at the cell surface through use of a dense silica support results in increased transfection [31]. In essence mechanisms that improve cell microcapsule contact could facilitate cell entry and combining cell interaction approaches may have additive or synergistic effects on cell delivery.

There is a growing interest in the idea of magnetically targeted delivery. Magnetofection has become an established *in vitro* method for the delivery of plasmid DNA to cells [32] and recent studies have demonstrated magnetically targeted gene transfection *in vivo* using magnetic liposomes [33] or microbubbles [34]. Although magnetically targeted drug delivery is an area of great interest [35] the potential for delivery of therapeutic proteins has not been explored. There have been reports on the cellular delivery of BSA with both magnetic nanoparticles [36] and magnetic microspheres[37] but we are not aware of any previous reports on delivery of bioactive protein to cells. The potential to use LbL microcapsules for magnetically targeted delivery of protein therapeutics offers a novel approach that would be suited to intracellularly acting molecules. Toxins could be a particularly suitable cargo if their positioning in microcapsules could also render them inactive until appropriate delivery in cells. Furthermore, the potential to deliver both protein and DNA cargoes in a magnetically targeted manner and from the same microcapsule illustrates the uniqueness and versatility of the LbL microcapsule delivery approach.

The demonstration of navigated microcapsules with consequent cell delivery to targeted cells is an important observation of this study. We know that microcapsules can be targeted with magnetism [13, 14] but here we show that cell delivery of two cargoes is dramatically enhanced when microcapsules are targeted with a magnet. The improved delivery is a consequence of the increased microcapsule to cell ratio at the site of the magnet. For targeted delivery of luciferase the concentration effect was two fold in area and the increase in activity was of the same degree. Similarly, the concentration in the transfection experiment was 5.4 fold in area, and the increase in light emission was approximately 7 fold when compared to the rest of the well. Clearly navigation increases the ratio of microcapsules per cell but our toxicity data suggests that there are limits to the extent to which this concentration can be safely performed. Other studies have also noted cellular toxicity of Fe_3O_4 nanoparticles [38, 39] which was associated with increased intracellular production of reactive oxygen species (ROS) along with cytoplasmic vacuolation, mitochondrial swelling and increased nitric oxide production. An interesting observation with Fe_2O_3 nanoparticles was that the oxidative stress could be prevented by treatment with ROS inhibitors [40], in LbL microcapsules, inhibitors could potentially be introduced into the capsule structure.

In terms of navigation we know that a magnetic field can be used to navigate microcapsules under flow conditions [11], so this raises the possibility that systemic *in vivo* delivery with magnetic targeting is feasible with guidance by magnetic resonance as shown by Pouponneau *et al* [41]. A prerequisite will be to assess the suitability of LbL microcapsules for intravenous delivery but success with similarly sized microbubbles suggests that intravascular delivery of with LbL microcapsules will be feasible.

Although we have demonstrated improved delivery of bioactive molecules alone and their targeted delivery with a magnet there is the potential to further enhance magnetic delivery through the use of an alternating magnetic field. Potentially magnetic nanoparticles within the microcapsule structure will vibrate in an alternating magnetic field and thus increase the permeability of microcapsules or cause hyperthermic heating both of which will promote cargo release. Other studies have demonstrated these effects with magnetic nanoparticles in microcapsule layers [42-44].

This study further informs us about the design of microcapsules for the delivery of bioactive molecules. The middle layer which we have previously shown to be redundant for delivery of

 This journal is © The Royal Society of Chemistry 2012

bioactive molecules [21] is shown here to be effectively used for inclusion of a physical property without impeding delivery of the bioactive cargo from the capsule core. Indeed the combination of functionalities (PEI coating for entry/endosomal escape promoter; magnetism for targeting/entry) in microcapsules enhances the delivery. With further scope for combining biological and physical activities, LbL assembled microcapsules offer an increasingly multifunctional delivery approach for bioactive molecules which differentiates them from other cell delivery systems.

Conclusions

In this work, intracellular delivery of an encapsulated enzyme and plasmid DNA with magnetic microcapsules was studied. Inclusion of magnetite nanoparticles in LbL microcapsules promoted enzyme and plasmid delivery to cells as a result of their more rapid sedimentation rate and improved contact with cells. In addition, magnetic microcapsules could be efficiently navigated to cells with a magnet located below the tissue culture well. In these guided experiments enhanced activity was delivered to cells with both enzyme and DNA containing LbL microcapsules.

Acknowledgements

This work was supported by an MRC pump prime discipline bridging initiative "Delivery of bioactive molecules with polyelectrolyte nanoparticles", EPSRC seed funding cross-disciplinary project "Optimizing Nanoengineered Capsules for Delivery of Medicines". The study was also supported by Russian government (grant No. 14.Z50.31.0004 to support scientific research projects implemented under the supervision of leading scientists at Russian institutions and Russian institutions of higher education). A. P. was funded by the SEMS DTA studentship programme and BBSRC "Targeted drug delivery to neurons and glia using light-and field-sensitive microcapsules" research grant. S.G. was funded by Nuffield Foundation Undergraduate Research Bursary of Royal Academy of Engineering.

Funding Sources

Medical Research Council, Engineering and Physical Sciences Research, Biotechnology and Biological Sciences Research Council, Royal Academy of Engineering, Russian Government.

Notes and references

[a] School of Engineering & Materials Science, Queen Mary University of London, London, E1 4NS, U.K.

[b] Saratov State University, 83 Astrakhanskaya Street, Saratov, 410012, Russia.

[c] Bone & Joint Research Unit, William Harvey Research Institute, Queen Mary University of London, London, EC1M 6BQ, U.K.

[†] These authors contributed equally.

[*] Corresponding author: e-mail: g.sukhorukov@qmul.ac.uk, Fax: + 44 (0) 20 8981 9804, Tel +44 (0)20 7882 5508.

References

1. I. Drachuk, M. K. Gupta and V. V. Tsukruk, *Advanced Functional Materials*, 2013, 23, 4437-4453.
2. V. P. Torchilin, *Annual review of biomedical engineering*, 2006, 8, 343-375.
3. V. Torchilin, *Drug discovery today. Technologies*, 2008, 5, e95-e103.
4. X. Dan, H. Zhenhua, S. Jing, W. Fei and Y. Weien, *Nano-Micro Letters*, 2012, 4, 118-123.
5. A. Fu, R. Tang, J. Hardie, M. E. Farkas and V. M. Rotello, *Bioconjug Chem*, 2014, 25, 1602-1608.
6. L. J. De Cock, S. De Koker, B. G. De Geest, J. Grooten, C. Vervaet, J. P. Remon, G. B. Sukhorukov and M. N. Antipina, *Angew Chem Int Ed Engl*, 2010, 49, 6954-6973.
7. G. B. Sukhorukov and H. Mohwald, *Trends Biotechnol*, 2007, 25, 93-98.
8. A. G. Skirtach, A. A. Antipov, D. G. Shchukin and G. B. Sukhorukov, *Langmuir*, 2004, 20, 6988-6992.
9. A. Muñoz Javier, P. del Pino, M. F. Bedard, D. Ho, A. G. Skirtach, G. B. Sukhorukov, C. Plank and W. J. Parak, *Langmuir*, 2008, 24, 12517-12520.
10. A. M. Pavlov, A. V. Sapelkin, X. Huang, M. P'Ng K, A. J. Bushby, G. B. Sukhorukov and A. G. Skirtach, *Macromol Biosci*, 2011, 11, 848-854.
11. S. Carregal-Romero, M. Ochs, P. Rivera-Gil, C. Ganas, A. M. Pavlov, G. B. Sukhorukov and W. J. Parak, *J Control Release*, 2012, 159, 120-127.
12. M. Ochs, S. Carregal-Romero, J. Rejman, K. Braeckmans, S. C. De Smedt and W. J. Parak, *Angew Chem Int Ed Engl*, 2013, 52, 695-699.
13. D. A. Gorin, S. A. Portnov, O. A. Inozemtseva, Z. Luklinska, A. M. Yashchenok, A. M. Pavlov, A. G. Skirtach, H. Mohwald and G. B. Sukhorukov, *Phys Chem Chem Phys*, 2008, 10, 6899-6905.
14. M. Nakamura, K. Katagiri and K. Koumoto, *Journal of Colloid and Interface Science*, 2010, 341, 64-68.
15. Y. Wu, Z. Wu, X. Lin, Q. He and J. Li, *ACS Nano*, 2012, 6, 10910-10916.
16. Y. Wang, J. Zhang, H.-Z. Jia, J. Yang, S.-Y. Qin, C.-W. Liu, R.-X. Zhuo and X.-Z. Zhang, *Macromolecular Bioscience*, 2012, 12, 1321-1325.
17. T. A. Kolesnikova, G. G. Akchurin, S. A. Portnov, G. B. Khomutov, G. G. Akchurin, O. G. Naumova, G. B. Sukhorukov and D. A. Gorin, *Laser Physics Letters*, 2012, 9, 643.
18. A. M. Pavlov, B. G. De Geest, B. Louage, L. Lybaert, S. De Koker, Z. Koudelka, A. Sapelkin and G. B. Sukhorukov, *Advanced materials*, 2013, DOI: 10.1002/adma.201303287.
19. B. Zebli, A. S. Susha, G. B. Sukhorukov, A. L. Rogach and W. J. Parak, *Langmuir*, 2005, 21, 4262-4265.
20. A. Koutsokeras, N. Purkayashta, A. Rigby, M. C. Subang, M. Sclanders, S. Vessillier, L. Mullen, Y. Chernajovsky and D. Gould, *FASEB J*, 2014, 28, 373-381.
21. A. M. Pavlov, G. B. Sukhorukov and D. J. Gould, *J Control Release*, 2013, 172, 22-29.
22. D. J. Gould, C. Bright and Y. Chernajovsky, *Arthritis Res Ther*, 2004, 6, R103-113.
23. R. Sheparovych, Y. Sahoo, M. Motornov, S. Wang, H. Luo, P. N. Prasad, I. Sokolov and S. Minko, *Chemistry of Materials*, 2006, 18, 591-593.
24. D. V. Volodkin, A. I. Petrov, M. Prevot and G. B. Sukhorukov, *Langmuir*, 2004, 20, 3398-3406.
25. A. M. Pavlov, G. B. Sukhorukov and D. J. Gould, *Biomacromolecules*, 2013, 14, 608-612.
26. R. G. Smits, G. J. M. Koper and M. Mandel, *The Journal of Physical Chemistry*, 1993, 97, 5745-5751.
27. L. Kastl, D. Sasse, V. Wulf, R. Hartmann, J. Mircheski, C. Ranke, S. Carregal-Romero, J. A. Martinez-Lopez, R. Fernandez-Chacon,

W. J. Parak, H. P. Elsasser and P. Rivera Gil, *ACS Nano*, 2013, 7, 6605-6618.
28. M. Feughelman, R. Langridge, W. E. Seeds, A. R. Stokes, H. R. Wilson, C. W. Hooper, M. H. Wilkins, R. K. Barclay and L. D. Hamilton, *Nature*, 1955, 175, 834-838.
29. P. H. Von Hippel and J. D. McGhee, *Annual review of biochemistry*, 1972, 41, 231-300.
30. C. Ganas, A. Weiss, M. Nazarenus, S. Rosler, T. Kissel, P. Rivera Gil and W. J. Parak, *J Control Release*, 2014, 196, 132-138.
31. D. Luo and W. M. Saltzman, *Nat Biotechnol*, 2000, 18, 893-895.
32. F. Scherer, M. Anton, U. Schillinger, J. Henke, C. Bergemann, A. Kruger, B. Gansbacher and C. Plank, *Gene Ther*, 2002, 9, 102-109.
33. S. H. Hu, T. Y. Hsieh, C. S. Chiang, P. J. Chen, Y. Y. Chen, T. L. Chiu and S. Y. Chen, *Advanced healthcare materials*, 2014, 3, 273-282.
34. H. Mannell, J. Pircher, F. Fochler, Y. Stampnik, T. Rathel, B. Gleich, C. Plank, O. Mykhaylyk, C. Dahmani, M. Wornle, A. Ribeiro, U. Pohl and F. Krotz, *Nanomedicine*, 2012, 8, 1309-1318.
35. J. Chomoucka, J. Drbohlavova, D. Huska, V. Adam, R. Kizek and J. Hubalek, *Pharmacological research : the official journal of the Italian Pharmacological Society*, 2010, 62, 144-149.
36. X. Huang, X. Meng, F. Tang, L. Li, D. Chen, H. Liu, Y. Zhang and J. Ren, *Nanotechnology*, 2008, 19, 445101.
37. X. Luo, S. Liu, J. Zhou and L. Zhang, *Journal of Materials Chemistry*, 2009, 19, 3538-3545.
38. M. T. Zhu, Y. Wang, W. Y. Feng, B. Wang, M. Wang, H. Ouyang and Z. F. Chai, *J Nanosci Nanotechnol*, 2010, 10, 8584-8590.
39. M. T. Zhu, B. Wang, Y. Wang, L. Yuan, H. J. Wang, M. Wang, H. Ouyang, Z. F. Chai, W. Y. Feng and Y. L. Zhao, *Toxicology letters*, 2011, 203, 162-171.
40. K. Buyukhatipoglu and A. M. Clyne, *Journal of biomedical materials research. Part A*, 2011, 96, 186-195.
41. P. Pouponneau, J. C. Leroux, G. Soulez, L. Gaboury and S. Martel, *Biomaterials*, 2011, 32, 3481-3486.
42. Z. Lu, M. D. Prouty, Z. Guo, V. O. Golub, C. S. S. R. Kumar and Y. M. Lvov, *Langmuir*, 2005, 21, 2042-2050.
43. K. Katagiri, Y. Imai and K. Koumoto, *Journal of Colloid and Interface Science*, 2011, 361, 109-114.
44. S. Carregal-Romero, P. Guardia, X. Yu, R. Hartmann, T. Pellegrino and W. J. Parak, *Nanoscale*, 2015, 7, 570-576.

 This journal is © The Royal Society of Chemistry 2012